

Accurate Calculations of Binding, Folding, and Transfer Free Energies by a Scaled Generalized Born Method

Hariato Tjong and Huan-Xiang Zhou*

*Department of Physics and Institute of Molecular Biophysics, Florida State University,
Tallahassee, Florida 32306*

Received May 14, 2008

Abstract: The Poisson–Boltzmann (PB) equation is widely used for modeling solvation effects. The computational cost of PB has restricted its applications largely to single-conformation calculations. The generalized Born (GB) model provides an approximation at substantially reduced cost. Currently the best GB methods reproduce PB results for electrostatic solvation energies with errors at ~ 5 kcal/mol. When two proteins form a complex, the net electrostatic contributions to the binding free energy are typically of the order of 5 to 10 kcal/mol. Similarly, the net contributions of individual residues to protein folding free energy are < 5 kcal/mol. Clearly in these applications the accuracy of current GB methods is insufficient. Here we present a simple scaling scheme that allows our GB method, GBr⁶, to reproduce PB results for binding, folding, and transfer free energies with high accuracy. From an ensemble of conformations sampled from molecular dynamics simulations, five were judiciously selected for PB calculations. These PB results were used for scaling GBr⁶. Tests on the binding free energies of the barnase-barstar, GTPase-WASp, and U1A-U1hplI complexes and on the folding free energy of FKBP show that the effects of point mutations calculated by scaled GBr⁶ are accurate to within 0.3 kcal/mol of PB results. Similar accuracy was also achieved for the free energies of transfer for ribonuclease Sa and insulin from the crystalline phase to the solution phase at various pHs. This method makes it possible to thoroughly sample the transient-complex ensemble in predicting protein binding rate constants and to incorporate conformational sampling in electrostatic modeling (such as done in the MM-GBSA approach) without loss of accuracy.

1. Introduction

Electrostatic interactions make important contributions to fundamental properties such as protein binding free energy, protein folding stability, and protein solubility. Point mutations and variations of salt concentration and pH are often used to probe such contributions. Computational methods that reliably predict those energetic effects are highly desirable, both for elucidating the underlying physical principles and for protein design. Developing such methods is a formidable task, since the free energy of binding, for example, is a small difference between two large quantities, namely the free energy due to interactions within the complex in the solvent environment and the solvation energy of the

subunits in the unbound state. The effects of point mutations on the free energy of binding or folding are even smaller. The Poisson–Boltzmann (PB) equation^{1–8} has found great success in modeling electrostatic contributions to mutational effects on protein binding free energy^{9–12} and protein folding stability.^{13–15} We have also been able to use the PB equation to model the effects of salt and pH on protein solubility.^{16,17} However, the computational cost of solving the PB equation presents a major stumbling block.

There have been some efforts devoted to the development of fast PB methods.^{4,6} An alternative that holds great promise is the generalized Born (GB) model,¹⁸ which approximates the PB equation at substantially reduced computational cost. Considerable efforts have been invested in developing GB methods that would hold down the computational cost but have great accuracy in reproducing the PB results.^{19–26}

* Corresponding author phone: (850)645-1336; fax: (850)644-7244; e-mail: zhou@sb.fsu.edu.

The reduced computational cost of the GB model opens new avenues for more realistic modeling of electrostatic effects, such as the inclusion of protein conformational sampling.²⁷ However, the small magnitudes of electrostatic contributions to binding and folding free energies pose a challenging demand on the accuracy of calculations. To date, the errors of the best GB methods in reproducing PB solvation energies are about 0.5% in relative terms or roughly several kcal/mol in absolute terms.^{26,28} The scatter of these errors among different proteins also appears to be random.

The electrostatic contributions to protein–protein binding free energies typically have an order of magnitude of 10 kcal/mol.^{9,10} Therefore even the currently most accurate GB methods (when benchmarked against PB results) may be inadequate for predicting binding free energy. One idea for improving accuracy is to reparameterize GB methods against PB results. One such attempt was made in calculating protein–ligand binding free energy,²⁹ using PB results for a subset of ligands as training data, but the error (as measured against PB results) in that work was still relatively large, about 5 kcal/mol. In fact, our recently developed GB method, GBr⁶, has even smaller errors on protein–protein binding free energies (~1 kcal/mol for protein complexes studied here) without any reparameterization.²⁶

Here we take a different approach to GB reparameterization. The aim of the reparameterization is to allow for conformational sampling in electrostatic modeling. For each protein or protein complex, we generate an ensemble of conformations from molecular dynamics simulations. The raw GB result for the solvation energy of each conformation in the ensemble is calculated, and five conformations are selected to be representative of the variations in solvation energy of the ensemble. PB results for the solvation energies of the five representative conformations are then calculated and used for scaling the corresponding raw GB results. The scaling factor is finally applied to the rest of the conformation ensemble. Accuracy of the scaling method is assessed by comparing the scaled GB results and PB results for the whole ensemble. While the scaling method is applicable to any GB method, we report here results for GBr⁶. We refer to the reincarnation scaled GBr⁶ or sGBr⁶ in short. The promise of reparameterizing GB against PB results calculated for a small subset of conformations was demonstrated in an early study.³⁰

We test scaled GBr⁶ on a number of applications. Mutational and salt effects on the binding free energies are calculated for four protein–protein and protein–RNA complexes. To assess the accuracy of scaled GBr⁶ for calculating mutational effects on folding free energy, 26 mutants of the FK506-binding protein (FKBP) are studied. In addition, scaled GBr⁶ is used to calculate the pH dependence of solubility of two proteins, ribonuclease Sa and insulin.

As another important application, we use scaled GBr⁶ to calculate the electrostatic interaction energy of the transient complex along the protein–protein association pathway, which predicts the electrostatic enhancement of the protein binding rate.^{31–34} The transient complex consists of an ensemble of configurations, each of which presents a slightly

different relative separation and relative orientation between the two subunits in a complex. Four pairs of binding proteins are studied.

In all these applications, we show that the relevant small differences in electrostatic solvation energy obtained by scaled GBr⁶ are accurate to within 0.3 kcal/mol of the corresponding PB results. These diverse applications illustrate the wide utility of our GB scaling approach.

II. Theory

In previous studies, we have described the theoretical models for calculating electrostatic contributions to free energies of protein binding^{9,10} and folding,^{13,14} for calculating the electrostatic rate enhancement of protein binding,^{31–34} and for calculating the pH dependence of protein solubility.¹⁷ Here we give brief outlines of these models.

2.1. Binding Free Energy. When two proteins, A and B, bind to form a complex C, the electrostatic contribution to the binding free energy is calculated as

$$\Delta G_b = G_{el}(C) - G_{el}(A) - G_{el}(B) \quad (1)$$

where $G_{el}(X)$, $X = A, B$, or C , is the electrostatic free energy of molecule X . $G_{el}(X)$ can be decomposed into a Coulomb term and a solvation term:

$$G_{el}(X) = G_{Coul}(X) + G_{solv}(X) \quad (2)$$

By this decomposition, ΔG_b has a Coulombic component and a solvation component. These will be denoted as $\Delta G_{b,Coul}$ and $\Delta G_{b,solv}$, respectively. When a point mutation is introduced, ΔG_b can be calculated for the wild-type (wt) pair of proteins and for the mutant (mt) pair. The change in ΔG_b by the mutation is

$$\Delta \Delta G_b = \Delta G_b(mt) - \Delta G_b(wt) \quad (3)$$

2.2. Folding Free Energy. For protein folding, we are interested in mutational effects on the electrostatic contribution to the folding free energy. It is assumed that, in the unfolded state, individual residues do not interact, and hence the contributions of residues other than the one under mutation are the same in the wild-type protein and the mutant. (Residual charge–charge interactions in the unfolded state have been modeled previously.³⁵) Neglecting the electrostatic free energy of the “other” residues in the unfolded state (which does not affect the change in folding free energy by the mutation), the electrostatic contribution to the folding free energy is

$$\Delta G_f = G_{el}(\text{protein}) - G_{el}(\text{residue}) \quad (4)$$

where the two terms on the right-hand side represent the electrostatic free energies of the protein in the folded state and the residue under mutation, respectively. The solvation component of ΔG_f will be denoted as $\Delta G_{f,solv}$. The mutational effect on ΔG_f is given by

$$\Delta \Delta G_f = \Delta G_f(mt) - \Delta G_f(wt) \quad (5)$$

Notice that even $\Delta G_f(wt)$ is mutant-specific; we will come back to this point in subsection 3.4.

2.3. pH Dependence of Solubility. The effect of pH on protein solubility can be calculated from the pH dependence

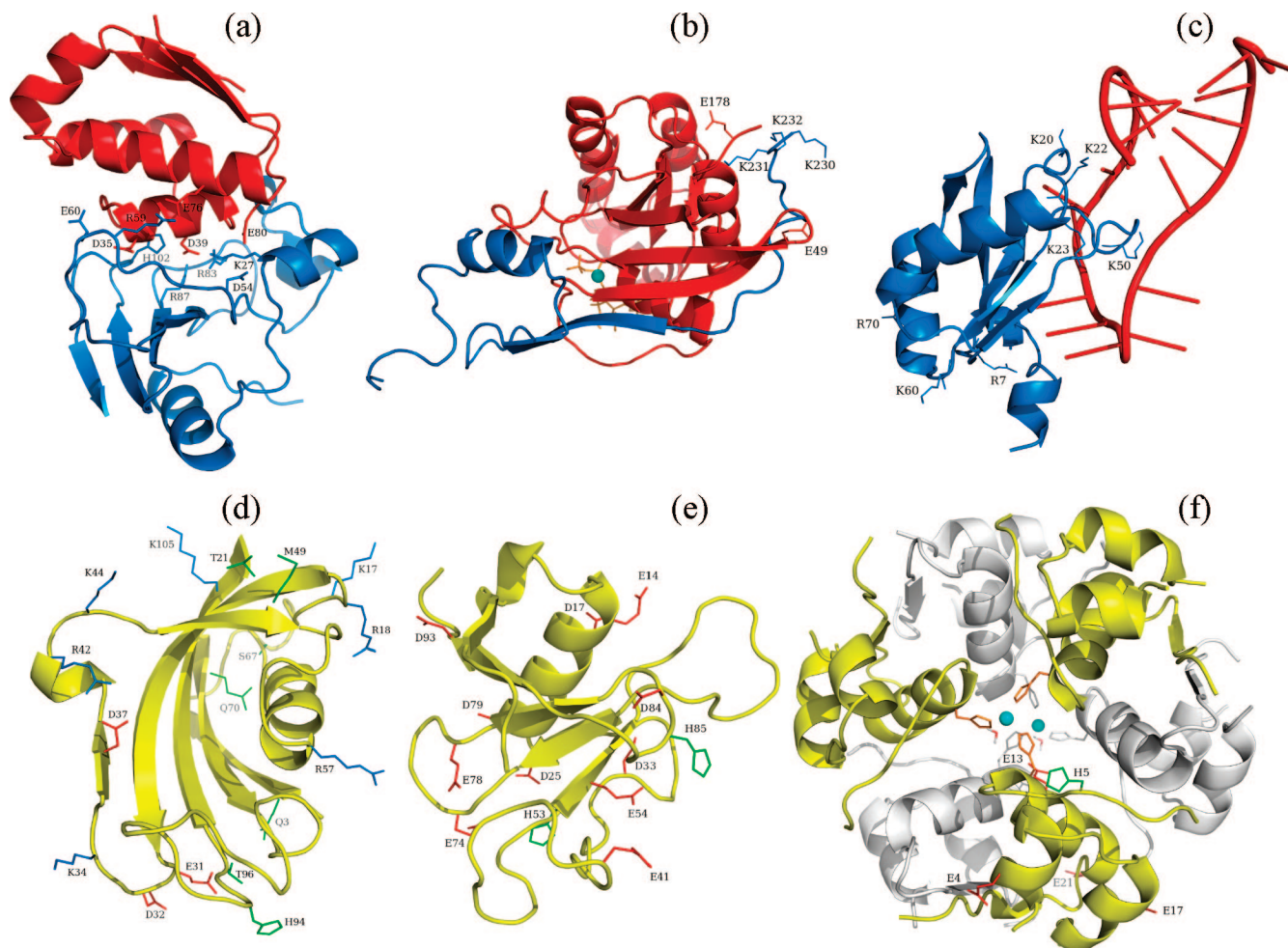


Figure 1. Systems studied in the present work. (a)–(c) Complexes of barnase and barstar, WASp and Cdc42, and U1A and U1SLII. The first and second subunits are shown in blue and red, respectively. (d) FKBP. (e) Ribonuclease Sa. (f) Insulin hexamer. Mutated residues in (a)–(d) and titrated residues in (e) and (f) are labeled.

of the transfer free energy of a protein from the condensed phase to the solution phase. Both the solution phase and the condensed phase are modeled as continuum dielectrics, with the dielectric constants taking a value appropriate for water (equal to 78.5 at room temperature) for the former and a value (~ 55) intermediate between those for water and for the protein solute. The electrostatic component of the transfer free energy, which is what is relevant for determining the pH dependence of solubility, is

$$\Delta G_t = G_{\text{solv}}(\epsilon_s = 78.5) - G_{\text{solv}}(\epsilon_s = 55) \quad (6)$$

where $G_{\text{solv}}(\epsilon_s)$ is the electrostatic solvation energy of the solute protein in a continuum solvent with dielectric constant ϵ_s . This result uses the fact that the Coulomb term is the same in both phases. $G_{\text{solv}}(\epsilon_s)$ at each pH was calculated by averaging over conformations sampled from constant-pH molecular dynamics simulations.

2.4. Electrostatic Rate Enhancement. According to the transient-complex theory,^{31,33,34} the rate constant for the association of two proteins under diffusion control can be predicted as

$$k_a = k_{a0} e^{-\Delta G_{\text{el}}^*/k_B T} \quad (7)$$

where k_{a0} is the basal rate constant, and ΔG_{el}^* is the electrostatic interaction energy of the proteins in the transient-

complex ensemble. ΔG_{el}^* is calculated as the average over configurations representing the transient complex. For each configuration, the electrostatic interaction energy is as defined by eq 1, except that C now represents a transient-complex configuration.

III. Computation Details

3.1. Generation of Conformational Ensembles. For calculating electrostatic contributions to protein binding and folding free energies by scaled GBr⁶, conformations were generated by explicit-solvent molecular dynamics (MD) simulations. Four protein–protein and protein–RNA complexes were studied: an enzyme–inhibitor complex formed by barnase and barstar; complexes formed by the Wiskott–Aldrich Syndrome protein (WASp) with two homologous Rho GTPases, Cdc42 and TC10; and a protein–RNA complex formed by the U1A protein and stem/loop II of the U1 small nuclear RNA (U1SLII). The first and last complexes were previously studied by PB calculations.^{9,11} The two GTPase–WASp complexes have been studied experimentally.³⁶ These and other systems studied here are shown in Figure 1.

The simulation of the barnase–barstar complex was carried out as follows. Starting from the X-ray structure of the complex (Protein Data Bank entry 1brs³⁷), hydrogens, four Na^+ ions as neutralizing counterions, and 9558 TIP3P water

molecules were added by the LEAP program in the Amber package.³⁸ The side chains of arginine and lysine residues were positively charged, side chains of aspartate and glutamate residues were negatively charged, and side chains of histidine residues were neutral (appropriate for a nominal pH of 7). The force field was ff99SB.³⁹ The solvent (water molecules plus counterions) was relaxed first by 200 steps of energy minimization and then by 100 ps of MD simulation at a constant pressure MD, all the while the protein complex was fixed. Next, the whole system was energy minimized with decreasing harmonic constraints applied to the protein complex, from 50 kcal/mol/Å² to 0, for a total of 2500 steps. The cutoff for the nonbonded interactions was 9 Å, and the particle mesh Ewald method was used to treat long-range electrostatic interactions. The whole system was then heated for 40 ps at constant volume to a final temperature of 298 K. Finally the simulation was continued at constant pressure and temperature. Bond lengths involving hydrogen atoms were restrained by the SHAKE algorithm⁴⁰ throughout the simulation, allowing a time step of 2 fs. The first 2 ns of the constant pressure and temperature simulation was discarded; thereafter conformations were sampled at every 10 ps, and a total of 548 conformations were collected.

For the Cdc42-WASp complex, an NMR structure with 20 models was available (Protein Data Bank entry 1cee).⁴¹ We randomly picked five (models 1, 5, 9, 13, and 17) of the 20 to generate conformational ensembles. No structure for the TC10-WASp complex was available. We modeled its structure by aligning the structure of unbound TC10 (Protein Data Bank entry 2atx³⁶) to Cdc42 in the five NMR models of the Cdc42-WASp complex. From these 10 starting structures (five for each complex), MD simulations were carried out following the protocol for the barnase-barstar complex. For each of the 10 simulations, 100 conformations were sampled at every 10 ps after discarding the first 1 ns of the constant pressure and temperature simulation.

The starting structure for the U1A-U1SLII complex was as prepared in our previous study.¹¹ 100 conformations were sampled at every 20 ps after discarding the first 2 ns of the constant pressure and temperature simulation.

FKBP was chosen as a model system for folding because it is a protein being studied experimentally in our laboratory.⁴² We have accumulated experimental data for the effects of a large number of charge mutations on the folding stability (J. Batra, HT, and HXZ, to be published). The same mutations are the targets of the present study. Starting from the X-ray structure (Protein Data Bank entry 1fkb⁴³), the MD simulation of FKBP followed the protocol for the barnase-barstar complex. 200 conformations were sampled at every 15 ps after discarding the first 1 ns of the constant pressure and temperature simulation.

Previously we have used PB calculations to predict the pH dependences of the solubility of two proteins, ribonuclease Sa and insulin.¹⁷ The transfer free energy from the condensed phase to the solution phase was calculated by averaging over conformations sampled from constant-pH MD simulations, which were based on the GB model.⁴⁴ For testing scaled GBr⁶, here we simply took the conformations generated in our previous work and used the PB results

calculated there as the benchmark. We just point out that 100 conformations were collected at each of the nine pH values (2.3, 2.9, 3.6, 4.0, 4.5, 4.8, 5.0, 5.2, and 5.4) for ribonuclease Sa and at each of the eight pH values (4.0, 4.5, 5.0, 5.5, 5.75, 6.25, 6.75, and 7.0) for insulin.

We have obtained PB results for the electrostatic interaction energies of the transient complexes of four protein pairs, formed by barnase and barstar, interleukin-4 (IL4) and interleukin-4 binding protein (IL4BP), colicin E9 and immunity protein 9 (Im9), and acetylcholinesterase (AChE) and fasciculin (fas).^{31–33} Each transient complex was represented by 100 configurations, generated by sampling in the six-dimensional space of relative translation and rotation (the conformations of the two subunits were held fixed). Here we used the same configurations and the PB results to test scaled GBr⁶.

3.2. Mutation Protocol. In the present work mutational effects on binding free energy were calculated for the barnase-barstar complex, the two GTPase-WASp complexes, and the U1A-U1SLII complex. Similarly mutational effects on folding free energy were calculated for FKBP. Mutations were modeled on each of the conformations collected from MD simulations of a “wild-type” protein or protein complex, and the protocol for mutation was the same as developed previously in single-conformation studies.^{9,11,13,14} Briefly, for each single mutation, the LEAP program was used to replace the wild-type side chain with the mutant side chain. The new side chain was then energy minimized in vacuum (while holding the rest of protein or protein complex fixed) up to 50,000 steps. Multiple mutations were decomposed into a series of single mutations.

The 17 mutations on the barnase-barstar complex studied previously⁹ were also the target of the present work. Of these, 11 are single mutations (bnK27A, bnD54A, bnR59A, bnE60A, bnR83Q, bnR87A, bnH102A, bsD35A, bsD39A, bsE76A, and bsE80A; bn and bs refer to barnase and barstar, respectively). The remaining 6 are double mutations (bnK27A/bsD39A, bnR59A/bsD35A, bnR59A/bsE76A, bnR59A/bsE80A, bnR83Q/bsD39A, and bnR87A/bsD39A). Similarly, seven single mutations (R7Q, K20Q, K22Q, K23Q, K50A, K60Q, and R70Q) on the U1A in its complex with U1SLII, studied previously,¹¹ were the target of the present work.

For the Cdc42-WASp complex, the present study covered a total of 10 mutations. Of these, 7 were single mutations (E49K on Cdc42, K230A, K230E, K231A, K231E, K232A, and K232E on WASp), 1 was a double mutation (E49K/E178K on Cdc42), and 2 were triple mutations (K230A/K231A/K232A and K230E/K231E/K232E on WASp). Two mutations were studied on the TC10-WASp complex: K63E and K63E/T192E; both are on TC10. For the purpose of making error assessment on scaled GBr⁶, we group together the 12 mutations on the two related GTPase-WASp complexes.

We studied 26 mutations on FKBP to find their effects on the folding free energy. These include 17 single, 5 double, 2 triple, 1 quadruple, and 1 quintuple mutation (listed in Figure 6).

3.3. PB and GB Calculations. The PB results for benchmarking scaled GBr⁶ on pH dependence of protein solubility and on electrostatic interaction energy of transient

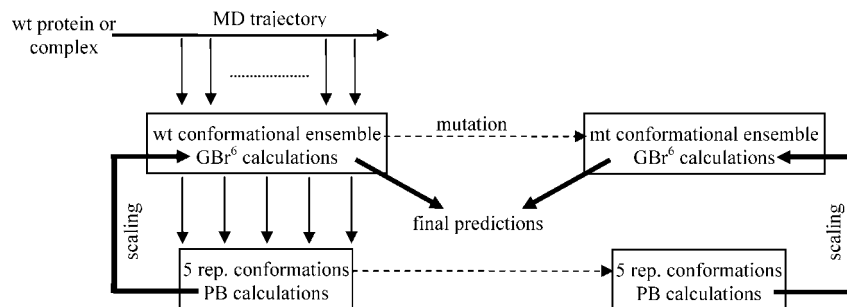


Figure 2. Illustration of the scaling protocol.

complex were available from previous studies.^{17,32} PB results for electrostatic contributions to binding and folding free energies were newly calculated here on the conformational ensembles described above. The calculations were done by the UHBD program² following a previously established protocol.^{9,11,13,14} In particular, the dielectric boundary between the protein or RNA low dielectric and the solvent high dielectric was specified by the van der Waals surface instead of the more popularly used molecular surface. We have had the most success with the former surface in comparing PB calculations with experimental results for mutational effects on protein folding and binding free energies^{9–11,13,14} and for electrostatic enhancement of protein binding rates.^{33,34} The van der Waals surface is also what is modeled into our GB method, GBr^6 .²⁶

Mutational effects on the barnase-barstar binding free energy were calculated for an ionic strength of 25 mM. In addition, PB and GB calculations were also carried out for the wild-type complex at ionic strengths of 50, 125, 225, 325, 525, and 1000 mM to test scaled GBr^6 on salt effects. The ionic strengths for PB and GB calculations were 100 mM for the GTPase-WASp complexes, 160 mM for the U1A-U1SLII complex, and 150 mM for FKBP. All calculations used the Amber94 atomic partial charges⁴⁵ and Bondi radii (H, 1.2 Å; O, 1.5 Å; N, 1.55 Å; C, 1.7 Å; S and P, 1.8 Å).⁴⁶ Except for the U1A-U1SLII complex, all PB results were obtained by solving the linearized PB equation. For the protein-RNA complex, the full PB equation was solved due to the high charges on the system. We have developed a version of GBr^6 called GBr^6NL ,⁴⁷ which mimics the full nonlinear PB equation. However, since the nonlinear PB equation has not been modeled by other GB methods and our scaling-based reparameterization was intended for GB methods in general, even for the U1A-U1SLII complex we used raw GBr^6 results for scaling. (We did use the nonlinear PB results for the U1A-U1SLII complex to test the scaling method on GBr^6NL . As expected, the raw GBr^6NL results had slightly less deviations from the PB targets than the raw GBr^6 results, but the scaling method worked equally well for the two GB versions.)

3.4. GB Scaling Protocol. Rather than refine GBr^6 internally, our strategy for reparameterization was to take raw GBr^6 results and postprocess them by scaling. The scaling was based on PB results for a small number (five) of conformations judiciously selected as representatives of the conformation ensemble. The selection varied somewhat from application to application, but followed the same overall design, as illustrated in Figure 2.

Let us illustrate the scaling protocol using mutational effects on the binding free energy of a protein complex. First, for each conformation in the ensemble, the raw GBr^6 result for $\Delta G_b(\text{wt})$ was calculated. Then, five conformations were selected for scaling purpose, based on the mean (m) and standard deviation (σ) of the raw GBr^6 results within the conformational ensemble. The representative conformations had raw GBr^6 results closest to the following target values: m , $m \pm 0.5\sigma$, $m \mp 0.75\sigma$, $m \pm 1.0\sigma$, and $m \mp 1.5\sigma$. The first or second set of signs was chosen depending on whether the actual value of the first conformation was above or below m . Other target values were experimented with, but the above values resulted in the best overall performance. We now refer to the raw GBr^6 results for the solvation component of $\Delta G_b(\text{wt})$ as $\Delta G_{\text{GB}}(i)$, $i = 1$ to 5, for the five conformations.

The corresponding PB results, $\Delta G_{\text{PB}}(i)$, $i = 1$ to 5, for the five representative conformations were also obtained. The average of the five individual ratios, $\Delta G_{\text{PB}}(i)/\Delta G_{\text{GB}}(i)$, was finally taken as the factor (λ) for scaling the raw GBr^6 results of the whole conformational ensemble. The same five representative conformations were also used for calculating the scaling factors of all mutants of the same protein complex. For each mutant, calculating the scaling factor involved again obtaining PB results on the five representative conformations. The ratio $\Delta G_{\text{PB}}(i)/\Delta G_{\text{GB}}(i)$ could spuriously deviate significantly from 1 when the magnitudes of $\Delta G_{\text{b,solv}}$ calculated by GBr^6 or PB on the representative conformations were too small. To prevent the scaling factor from being biased by such spurious ratios, we filtered out ratios outside the range of 0.75 to 1.25. This filtering was triggered only rarely in the present study.

After the scaling factors were separately found for the wild-type complex and each mutant, the mutational effect on the electrostatic contribution to the binding free energy was calculated as

$$\Delta\Delta G_b = [\lambda(\text{mt})\Delta G_{\text{GB}}(\text{mt}) + \Delta G_{\text{b,Coul}}(\text{mt})] - [\lambda(\text{wt})\Delta G_{\text{GB}}(\text{wt}) + \Delta G_{\text{b,Coul}}(\text{wt})] \quad (8)$$

This equation was applied to the individual conformations in the ensemble, all using the same scaling factors $\lambda(\text{mt})$ and $\lambda(\text{wt})$. The final, ensemble-averaged, prediction for the mutational effect was taken as an average of the results for $\Delta\Delta G_b$ calculated on the individual conformations. The same procedure was also adopted for studying salt effects on the binding free energy. In that case ‘mt’ and ‘wt’ refer to the salt concentration of interest and a reference salt concentration, respectively.

Table 1. PB, sGBr⁶, and Experimental Results (in kcal/mol) for $\Delta\Delta G_b$ of 17 Mutations on the Barnase-Barstar Complex^a

mutants	PB range	PB m \pm sd	sGBr ⁶ m \pm sd	expt
bnK27A	3.97 to 6.77	5.28 \pm 0.50	5.34 \pm 0.43	5.4
bnD54A	-2.93 to -1.36	-2.05 \pm 0.26	-1.91 \pm 0.17	-0.9
bnR59A	3.11 to 6.52	4.82 \pm 0.57	4.89 \pm 0.53	5.2
bnE60A	-1.40 to 0.65	-0.52 \pm 0.35	-0.31 \pm 0.36	-0.3
bnR83Q	4.08 to 8.82	6.72 \pm 0.61	6.69 \pm 0.57	5.4
bnR87A	3.89 to 6.20	4.91 \pm 0.43	4.84 \pm 0.39	5.5
bnH102A	0.28 to 2.39	1.50 \pm 0.34	1.55 \pm 0.36	6.1
bsD35A	2.17 to 6.13	3.82 \pm 0.72	3.92 \pm 0.61	4.5
bsD39A	5.56 to 10.32	7.97 \pm 0.83	8.05 \pm 0.79	7.7
bsE76A	1.92 to 4.83	3.35 \pm 0.54	3.37 \pm 0.52	1.4
bsE80A	-0.16 to 0.95	0.38 \pm 0.18	0.39 \pm 0.13	0.5
bnK27A/bsD39A	6.93 to 11.25	9.24 \pm 0.83	9.25 \pm 0.75	8.2
bnR59A/bsD35A	4.27 to 9.71	7.02 \pm 0.89	7.03 \pm 0.80	6.3
bnR59A/bsE76A	2.97 to 6.39	4.63 \pm 0.58	4.68 \pm 0.53	4.9
bnR59A/bsE80A	2.99 to 6.47	4.74 \pm 0.60	4.88 \pm 0.54	5.1
bnR83Q/bsD39A	6.93 to 11.68	9.36 \pm 0.92	9.33 \pm 0.91	6.4
bnR87A/bsD39A	5.88 to 10.52	8.17 \pm 0.86	8.20 \pm 0.80	7.1

^a PB and sGBr⁶ results were calculated on 548 conformations sampled from an MD simulation. Range, m, and sd refer to the range of variation, the mean, and the standard deviation, respectively, of $\Delta\Delta G_b$ among the conformations.

The scaling protocol for mutational effects on the folding free energy was similar. In this case, ΔG_f , as defined in eq 4, was used for scaling. As noted in subsection 2.2, even $\Delta G_f(\text{wt})$ is mutant-specific; therefore, unlike in the case of binding free energy, it is not possible to have one set of five representative conformations that is applicable to all mutants. Instead, for each mutant, the five representative conformations were selected based on GBr⁶ results for $\Delta G_f(\text{wt})$. The scaling factors for the wild-type protein and the mutant were then found by obtaining PB results for the solvation components of $\Delta G_f(\text{wt})$ and $\Delta G_f(\text{mt})$ on these five conformations.

Extensions of the scaling protocol to studies of pH dependence of protein solubility and electrostatic rate enhancement were straightforward. For the former we just mention that ΔG_t , the electrostatic component of the transfer free energy, was used for scaling. For the latter study, we mention that the interaction energy ΔG_{el}^* itself, as opposed to its changes by mutation or by salt, was of direct interest.

IV. Results and Discussion

4.1. Importance of Conformational Sampling. The premise of our method for GB reparameterization is that results calculated from an extensive conformational ensemble are much more reliable than those from a single conformation. It can be argued, from both fundamental and practical points of view, that a conformational ensemble is superior to a single conformation for predicting binding and folding free energies. In mimicking experimental measurements, an ensemble of conformations is obviously more realistic than a single conformation; experimental results are averages over a conformational ensemble under certain solvent conditions. In a statistical sense, the errors of calculation results decrease with increasing size of the conformational ensemble.

We use PB results for the effects of 17 mutations on the binding free energy of the barnase-barstar complex to illustrate the comparison between ensemble and single-conformation predictions. For each mutation, we take the mean value of the PB results for $\Delta\Delta G_b$ over the 548 sampled conformations as the ensemble prediction. The 548 conformations were sampled over the course of 5.5 ns of MD

simulation. The pairwise root-mean-square-deviations (rmsd) between C α atoms of the 548 conformations were peaked around 1 Å, typical of conformational fluctuations of structured proteins on the ns time scale. For all the mutants, the ranges of variation of $\Delta\Delta G_b$ within the conformational ensemble were found to be comparable to the magnitudes of the mean $\Delta\Delta G_b$ values (Table 1). For example, for the barnase R59A mutation, PB results for $\Delta\Delta G_b$ among the 548 conformations varied from 3.1 to 6.5 kcal/mol, spanning a range of 3.4 kcal/mol. In comparison, the mean $\Delta\Delta G_b$ is 4.8 kcal/mol, and the standard deviation is 0.6 kcal/mol. The fact that, relative to the mean value, the range of variation of $\Delta\Delta G_b$ is large whereas the standard deviation is small provides direct evidence that the ensemble prediction is much more reliable than single-conformation predictions.

We further assess the ensemble and single-conformation predictions against experimental binding data for the 17 mutations (Table 1).^{48–50} For each single conformation, we measure prediction error by the root-mean-square-deviation (rmsd) between PB results for $\Delta\Delta G_b$ and experimental data for the 17 mutations. The errors calculated over the 548 sampled conformations are presented in Figure 3 as a histogram. They range from 1.25 to 2.27 kcal/mol. In comparison, the ensemble prediction has an rmsd of 1.55 kcal/mol from experiment. The latter value places the ensemble prediction in the 31st percentile of the single-conformation predictions. In other words, the probability of a randomly chosen single conformation performing worse than the ensemble is 69%. We thus show that, relative to single-conformation predictions, the ensemble prediction is not only more precise (as measured by standard deviation of the ensemble) but also more accurate (as measured by rmsd from experiment).

4.2. Performance of Raw GBr⁶. To establish a baseline for assessing the performance of scaled GBr⁶, we first benchmark the original GBr⁶ against PB. For each $\Delta\Delta G_b$, $\Delta\Delta G_f$, ΔG_t , or ΔG_{el}^* value, we take the ensemble-averaged PB result as the target and measure error as the deviation of the ensemble-averaged GBr⁶ result from the PB target. When multiple mutants on the same protein or protein complex

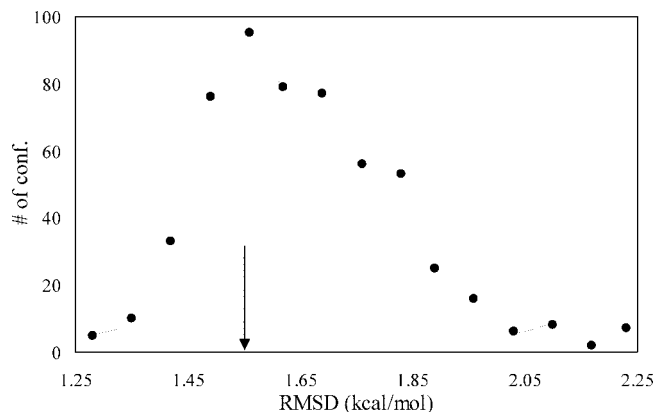


Figure 3. Distribution of PB-experiment difference among 548 conformations of the barnase-barstar complex. On each conformation, PB results for $\Delta\Delta G_b$ of 17 mutations were obtained, and their rmsd from experiment was used as the measure of PB-experiment difference. A vertical arrow, at 1.55 kcal/mol, indicates the rmsd of the ensemble prediction.

are studied (for $\Delta\Delta G_b$ and $\Delta\Delta G_f$ results), or when one protein is studied at different pH (for ΔG_t results), we report a single error value, which is given by the rmsd from the PB targets among all the mutants or all the pH values.

The errors of the original GBr⁶ for the various types of calculations are summarized in Table 2. For the barnase-barstar complex, $\Delta\Delta G_b$ errors calculated by GBr⁶ for the 17 individual mutations ranged from 0.1 to 1.9 kcal/mol, resulting in an overall rmsd of 0.85 kcal/mol. Similar $\Delta\Delta G_b$ errors are also seen for mutations on the GTPase-WASp and U1A-U1SLII complexes.

It is interesting to note that the $\Delta\Delta G_b$ errors seen on these complexes are suppressed by error cancellation between calculations on a complex and calculations on the separate subunits. For example, for the barnase R59A mutation, GBr⁶ overestimated the magnitude of the solvation energy of the complex by 2.22 kcal/mol and at the same time overestimated the magnitudes of the solvation energies of the two subunits by 2.61 and 0.05 kcal/mol, respectively. Taken together, the net error on $\Delta G_b(\text{mt})$ was only 0.44 kcal/mol. While this error cancellation was widely seen on the protein complexes studied here, there is no guarantee that it will always occur. It is possible that, for a given protein complex, GBr⁶ overestimates the solvation energy of the complex but at the same time underestimates the solvation energies of the subunits. In that situation, the errors accumulate rather than cancel. Errors from calculations on a mutant and those on the wild-type complex may also either cancel or accumulate. For the barnase R59A mutation, GBr⁶ errors on $\Delta G_b(\text{mt})$ and $\Delta G_b(\text{wt})$ occurred in opposite directions, resulting in an accumulative error of 0.64 kcal/mol on $\Delta\Delta G_b$. On the other hand, for the U1A-U1SLII complex, GBr⁶ errors on $\Delta G_b(\text{mt})$ and $\Delta G_b(\text{wt})$ occurred in the same direction; otherwise the differences in $\Delta\Delta G_b$ between GBr⁶ and PB, which was from solving the nonlinear PB equation for this particular complex, would have been much greater.

The $\Delta\Delta G_f$ errors calculated by GBr⁶ for the 26 individual mutations on FKBP reached as much as 2.4 kcal/mol. Even though the overall rmsd of 1.1 kcal/mol of all the 26

mutations is only slightly more than what was found above for the mutational effects on the binding free energy of the barnase-barstar complex, the $\Delta\Delta G_f$ errors on FKBP are much more significant. According to PB calculations (see Figure 6 below), of the 26 mutations, 9 changed the folding free energy of FKBP by less than 0.5 kcal/mol, and another 8 by 0.5 to 1.0 kcal/mol; the largest effect of an individual mutation was 3.5 kcal/mol. In contrast, as shown in Table 1 under the “PB $m \pm \text{sd}$ ” heading, only 2 of the 17 mutations on the barnase-barstar complex affected the binding free energy by less than 1.0 kcal/mol; the largest effect of an individual mutation was 9.4 kcal/mol.

The ΔG_t results calculated by GBr⁶ for ribonuclease Sa at nine pH values deviated from their PB targeted by 0.2 to 0.9 kcal/mol, resulting in an overall rmsd of 0.46 kcal/mol. Deviations of such magnitudes are significant because the PB results at the nine pH values differed at most by only 1.3 kcal/mol, and it is these small differences that predict the pH dependence of the solubility.¹⁷ For insulin, the deviations of GBr⁶ results for ΔG_t results at eight pH values were quite large, ranging from 2.5 to 9.3 kcal/mol (with an rmsd of 6.8 kcal/mol). The larger deviations most likely were due to the large size of the insulin hexamer (with a total of 306 residues); our GBr⁶ method was benchmarked on a set of proteins with up to 250 residues.²⁶

In our previous study,³² the PB results for ΔG_{el}^* calculated on the transient-complex ensembles of the barnase-barstar, IL4-IL4BP, E9-Im9, and AChE-fas protein pairs were -3.3 , -4.3 , -3.1 , and -4.0 kcal/mol, respectively. The corresponding GBr⁶ results obtained here were -0.45 , -1.4 , -0.73 , and 0.57 kcal/mol, respectively. The raw GBr⁶ results thus had large errors.

While the ensemble-averaged values of $\Delta\Delta G_b$, $\Delta\Delta G_f$, ΔG_t , and ΔG_{el}^* obtained by GBr⁶ had relatively large deviations from the PB targets, in each application the GBr⁶ and PB sets of values calculated on the individual conformations did show strong correlations. In Figure 4 we illustrate the correlations on the E49K/E178K mutation of Cdc42 for binding and on the T21K mutation of FKBP for folding. From linear regression analyses with the requirement of a zero intercept, the correlation R^2 values were ~ 0.99 . The strong correlations between raw GBr⁶ results and their PB counterparts are the foundation of our scaling-based GB reparameterization. The errors of raw GBr⁶ are manifested by a nonunity slope of the GBr⁶–PB correlation, which, as will be seen shortly, is rectified by the scaling.

4.3. Performance of Scaled GBr⁶. Upon applying scaling factors calculated on a small subset of five conformations, the errors of GBr⁶ on $\Delta\Delta G_b$, $\Delta\Delta G_f$, ΔG_t , and ΔG_{el}^* all dropped to within 0.3 kcal/mol (Table 2). Just like in the previous subsection, errors refer to deviations from the PB targets. For the barnase-barstar complex, the errors of scaled GBr⁶ for 13 of the 17 mutations were less than 0.1 kcal/mol, and the errors of the remaining 4 mutations were less than 0.2 kcal/mol; the overall rmsd was 0.09 kcal/mol. Notice that the latter value is much smaller than the fluctuations of the PB results for $\Delta\Delta G_b$ within the conformational ensemble (see Table 1). The final predictions of scaled GBr⁶ for $\Delta\Delta G_b$ are given in Table 1 for comparison against experimental

Table 2. Errors of Raw GBr⁶ and sGBr⁶ as Measured by Deviations from PB Results^a

system	no. of conf.	no. of mt or pH ^b	PB results	GBr ⁶ error	sGBr ⁶ error
$\Delta\Delta G_b$					
Bn-Bs	548	17	-2.1 to 9.4	0.85	0.09
GTPase-WASp #1	100	12	-1.2 to 7.9	1.12	0.14
GTPase-WASp #5	100	12	-1.9 to 7.2	1.28	0.19
GTPase-WASp #9	100	12	-1.8 to 8.6	0.95	0.20
GTPase-WASp #13	100	12	-1.5 to 8.3	1.30	0.32
GTPase-WASp #17	100	12	-3.1 to 6.7	1.30	0.32
U1A-U1SLII	100	7	0.1 to 3.1	0.69	0.05
$\Delta\Delta G_f$					
FKBP	200	26	-3.5 to 1.4	1.11	0.14
ΔG_t					
RNase Sa	100	9	-13.8 to -12.5	0.46	0.07
insulin	100	8	-63.2 to -60.9	6.83	0.34
ΔG_{el}^*					
Bn-Bs	100		-3.30	2.85	0.07
IL4-IL4BP	100		-3.05	2.94	0.22
E9-Im9	100		-4.33	2.32	0.07
AChE-fas	100		-4.04	4.61	0.06

^a All are in kcal/mol. ^b In $\Delta\Delta G_b$ and $\Delta\Delta G_f$ calculations, multiple mutations on a given protein or protein complex were studied. Error was measured by rmsd among the mutations. In ΔG_t calculations, a given protein was studied at multiple pH values; again rmsd was used as the measure of error.

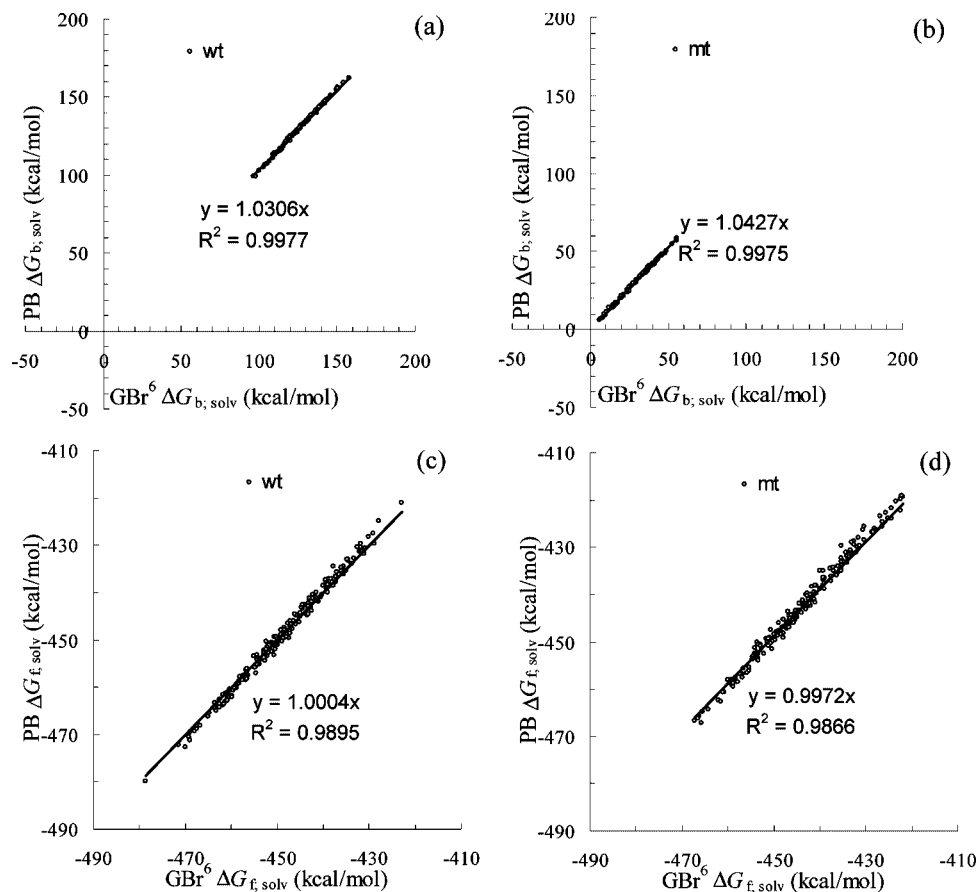


Figure 4. Correlation of GBr⁶ and PB results for $\Delta G_{b,solv}$ ($\Delta G_{f,solv}$), the solvation component of the electrostatic contribution to the binding (folding) free energy. Both sets of results were calculated on the same conformational ensemble. (a) and (b) $\Delta G_{b,solv}$ of wild-type Cdc42-WASp complex and the Cdc42 E49K/E178K mutant. (c) and (d) $\Delta G_{f,solv}$ of wild-type FKBP and the T21K mutant. In the linear regression analyses, the y-intercepts were always constrained at zero.

and PB results. The rmsd of scaled GBr⁶ results from experiment was 1.53 kcal/mol, virtually the same as the 1.55-kcal/mol rmsd of PB results from experiment. We further tested scaled GBr⁶ for predicting salt effects on the binding

free energy of the barnase-barstar complex. According to PB calculations, increasing ionic strength from 25 mM to 1 M reduces the magnitude of the binding free energy by 2.2 kcal/mol. As Figure 5 shows, scaled GBr⁶ remarkably well

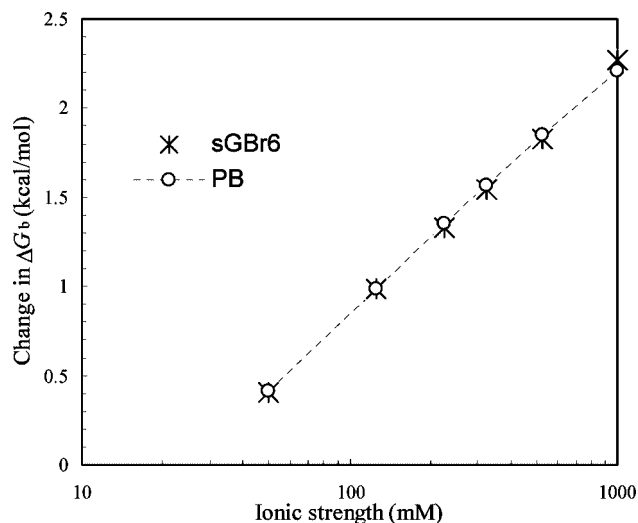


Figure 5. Comparison of scaled GBr⁶ and PB results for the salt dependence of the barnase-barstar binding free energy. Changes in ΔG_b from the respective results at an ionic strength of 25 mM are displayed.

reproduces the salt dependence of the binding free energy obtained by PB.

Very good agreement between scaled GBr⁶ and PB was also observed for the GTPase-WASp complexes. As summarized in Table 2, the RMSDs of scaled GBr⁶ from PB, calculated over 12 mutations on the two related complexes, ranged from 0.14 to 0.32 kcal/mol among conformational ensembles sampled using five different NMR models as starting structures. The average rmsd over the five conformational ensembles was 0.23 kcal/mol.

The highly charged protein-RNA complex between U1A and U1SLII did not present an obstacle for the scaling method. The rmsd between scaled GBr⁶ and PB was just 0.05 kcal/mol among seven mutations. Note that for this system the PB results were obtained from solving the nonlinear PB equation, so the test on this system demonstrates that scaled GBr⁶ can work well even for highly charged systems such as protein-nucleic acid complexes, for which the nonlinear PB equation would otherwise be required. Solving the full nonlinear PB equation takes much longer CPU time than solving the linearized version. For highly charged systems, scaled GBr⁶ affords especially significant gain in computational speed and yet can still be highly accurate for calculating small electrostatic effects such as those caused by mutations on binding free energy.

The success of scaled GBr⁶ with predicting binding free energy was repeated on predicting folding free energy. For 26 mutations on FKBP, the rmsd from PB targets was just 0.14 kcal/mol. A comparison between $\Delta\Delta G_f$ results obtained by scaled GBr⁶ and PB for the 26 mutations is displayed in Figure 6. Note that scaled GBr⁶ performed equally well for single mutations and for multiple mutations. Once again the deviations of GBr⁶ from PB are much smaller than the fluctuations of the PB results for $\Delta\Delta G_f$ within the conformational ensemble.

Let us use a binding example and a folding example to illustrate how scaled GBr⁶ achieved its accuracy. The binding example is the E49K/E178K mutation of Cdc42, and the

folding example is the T21K mutation of FKBP. The correlations between raw GBr⁶ and PB for these two examples have been shown in Figure 4. For binding, the slope of the linear regression between raw GBr⁶ and PB was 1.0306 for the wild-type complex and 1.0427 for the mutant. The optimal scaling would be to use these slopes as scaling factors. However, obtaining these slopes would require PB results for the whole conformational ensemble, which defeats the purpose of designing GB methods. By using PB results for a small subset of five conformations, we obtained scaling factors of 1.0306 for the wild-type complex and 1.0403 for the mutant. These scaling factors are very close to the slopes from linear regression, hence explaining why scaled GBr⁶ was so accurate. Similarly, for the folding examples, the slopes from linear regression were 1.0004 for wild-type FKBP and 0.9972 for the mutant. For the subset of five conformations, the scaling factors were found to be 1.0016 for the wild-type protein and 0.9982 for the mutant. The latter pairs of values again are very close to the respective slopes.

Raw GBr⁶ already did a good job in reproducing PB for ΔG_f of ribonuclease Sa. Scaling was able to further reduce the rmsd, from 0.46 to 0.07 kcal/mol, among nine pH values. For insulin, scaled GBr⁶ dramatically reduced the error on ΔG_b , from 6.8 to 0.34 kcal/mol. For ΔG_{el}^* of the four protein pairs, scaling was able to essentially erase the large errors of raw GBr⁶. Scaled GBr⁶ results differed from the PB targets by 0.2 kcal/mol or less for all four protein pairs.

We carried out some experimentation with the number of representative conformations used for calculating scaling factors. Our conclusion is that five is the optimal compromise between accuracy (demanding more conformations) and computational cost (demanding less conformations). However, it seems that even with fewer numbers of conformations, the performance of scaled GBr⁶ will not deteriorate significantly. In our test on the barnase-barstar complex, using only three representative conformations (the first, second, and third, or the first, third, and last of the original five), the rmsd between scaled GBr⁶ and PB increased only minutely, from 0.09 to 0.14 kcal/mol.

The success of scaled GBr⁶ in achieving very good agreement with PB results owes in large part to the quality of the original GBr⁶ results. As shown in Figure 4, the original GBr⁶ results have high linear correlations with PB results, and the y-intercepts of these correlations are nearly zero. In the early work of David et al.,³⁰ the GB method used produced significant y-intercepts, which were probably the main reason for the modest improvement achieved by reparameterization.

4.4. Cross-Validations. It is interesting to know how well the scaling scheme works when scaling factors obtained on five conformations selected from one subensemble are applied to another subensemble. As an example, an early portion of a MD trajectory may be used to generate the conformations for producing the scaling factors, which may then be applied to conformations sampled from the continuation of the MD simulation. To address the question posed above, we designed two types of cross-validation tests, depending on how the conformations were divided into subensembles. The barnase-barstar complex was chosen for

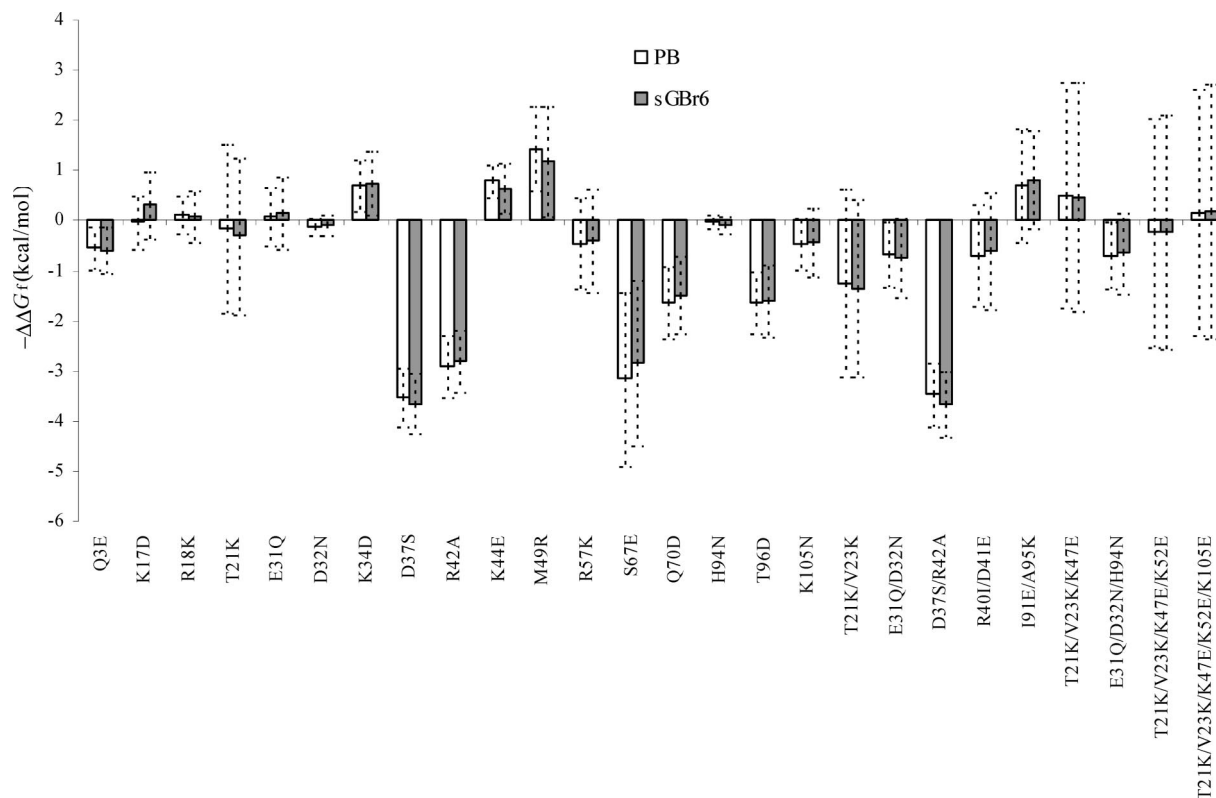


Figure 6. Comparison of scaled GBr⁶ and PB results for $\Delta\Delta G_r$ of 26 mutations on FKBP. Error bars indicate standard deviations within the conformational ensemble.

Table 3. Cross-Validation of sGBr⁶ on $\Delta\Delta G_b$. Results of 17 Mutations on the Barnase-Barstar Complex^a

training	type-1 test	type-2 test
subensemble 1	0.15 (0.08)	0.06 (0.06)
subensemble 2	0.09 (0.09)	0.15 (0.15)
subensemble 3	0.14 (0.16)	0.14 (0.14)
subensemble 4	0.14 (0.12)	0.12 (0.12)
average	0.13 (0.11)	0.12 (0.12)

^a Under each type of test, error in kcal/mol, as measured by rmsd from PB targets, is given. The number in parentheses represents the error when the scaling factors were applied to the training subensemble itself; the number outside represents the error obtained on the other three subensembles.

this purpose simply because it happened to have the most conformations (548) saved and PB results calculated for benchmarking. In the first cross-validation test, the 548 conformations were divided into four equal subensembles according to time sequence. In the second cross-validation test, every fourth conformation was collected into a subensemble, and each of the first four conformations of the whole ensemble started a different subensemble.

We refer to the subensemble from which the scaling factors were obtained as the training subensemble and examine whether the scaling factors when applied to a different subensemble would lead to larger errors than when applied to the training subensemble itself. As the results in Table 3 show, for both types of cross-validation tests, applying the scaling factors to the training or a different subensemble produces very similar errors.

A caveat about the cross-validation tests is that the different subensembles must all be part of the conformational fluctuations within a single deep energy well. If the protein

or protein complex undergoes a conformational transition and different subensembles are collected before and after the transition, cross validation clearly will fail. It is important that, in designing scaling schemes, such conformational transitions are recognized, and one set of scaling factors is used for each unique deep energy well.

V. Conclusion

We have demonstrated that a scaled GB method accurately reproduces PB results for binding and folding free energies, transfer energies between crystalline and solution phases, and electrostatic interaction energies in transient complexes. The scaled GB method thus opens the door to incorporate conformational sampling in robust and accurate modeling of small electrostatic effects, which fall within the error range of current GB methods.

The deviations of scaled GBr⁶ from PB are much smaller than the fluctuations of PB results within conformational ensembles. Our scaling scheme thus seems to have pushed GB methods to their accuracy limit. In our opinion, reparameterization without reference to any PB results will never be able to reach such a level of accuracy. Combining one of the most accurate raw GB methods with a PB-guided scaling method, scaled GBr⁶ promises to be a prototype for a new generation of fast continuum solvation models for incorporating conformational sampling in binding and folding free energy and other related calculations. A major application of GB methods is in implicit-solvent molecular dynamics simulations. Applying scaled GBr⁶ in such simulations is underway.

Acknowledgment. This work was supported in part by NIH grant GM058187.

References

- (1) Gilson, M. K.; Honig, B. Calculation of the total electrostatic energy of a macromolecular system: Solvation energies, binding energies, and conformational analysis. *Proteins* **1988**, *4*, 7–18.
- (2) Madura, J. D.; Briggs, J. M.; Wade, R.; Davis, M. E.; Luty, B. A.; Ilin, A.; Antosiewicz, J.; Gilson, M. K.; Bagheri, B.; Scott, L. R.; McCammon, J. A. Electrostatic and diffusion of molecules in solution: simulations with the University of Houston Brownian Dynamics program. *Comput. Phys. Commun.* **1995**, *91*, 57–95.
- (3) Baker, N. A.; Sept, D.; Joseph, S.; Holst, M. J.; McCammon, J. A. Electrostatics of nanosystems: application to microtubules and the ribosome. *Proc. Natl. Acad. Sci. U.S.A.* **2001**, *98*, 10037–10041.
- (4) Grant, J. A.; Pickup, B. T.; Nicholls, A. A smooth permittivity function for Poisson-Boltzmann solvation methods. *J. Comput. Chem.* **2001**, *22*, 608–640.
- (5) Fogolari, F.; Brigo, A.; Molinari, H. The Poisson-Boltzmann equation for biomolecular electrostatics: a tool for structural biology. *J. Mol. Recognit.* **2002**, *15*, 377–392.
- (6) Luo, R.; David, L.; Gilson, M. K. Accelerated Poisson-Boltzmann calculations for static and dynamic systems. *J. Comput. Chem.* **2002**, *23*, 1244–1253.
- (7) Lu, Q.; Luo, R. A Poisson-Boltzmann dynamics method with nonperiodic boundary condition. *J. Chem. Phys.* **2003**, *119*, 11035–11047.
- (8) Baker, N. A. Improving implicit solvent simulations: a Poisson-centric view. *Curr. Opin. Struct. Biol.* **2005**, *15*, 137–143.
- (9) Dong, F.; Vijayakumar, M.; Zhou, H.-X. Comparison of calculation and experiment implicates significant electrostatic contributions to the binding stability of barnase and barstar. *Biophys. J.* **2003**, *85*, 49–60.
- (10) Dong, F.; Zhou, H.-X. Electrostatic contribution to the binding stability of protein-protein complexes. *Proteins* **2006**, *65*, 87–102.
- (11) Qin, S.; Zhou, H.-X. Do electrostatic interactions destabilize protein-nucleic acid binding. *Biopolymers* **2007**, *86*, 112–118.
- (12) Bertonati, C.; Honig, B.; Alexov, E. Poisson-Boltzmann calculations of nonspecific salt effects on protein-protein binding free energies. *Biophys. J.* **2007**, *92*, 1891–1899.
- (13) Vijayakumar, M.; Zhou, H.-X. Salt bridges stabilize the folded structure of barnase. *J. Phys. Chem. B* **2001**, *105*, 7334–7340.
- (14) Dong, F.; Zhou, H.-X. Electrostatic contributions to T4 lysozyme stability: solvent-exposed charges versus semi-buried salt bridges. *Biophys. J.* **2002**, *83*, 1341–1347.
- (15) Tan, Y. H.; Luo, R. Protein stability prediction: a Poisson-Boltzmann approach. *J. Phys. Chem. B* **2008**, *112*, 1875–1883.
- (16) Zhou, H.-X. Interactions of macromolecules with salt ions: an electrostatic theory for the Hofmeister effect. *Proteins* **2005**, *61*, 69–78.
- (17) Tjong, H.; Zhou, H.-X. Prediction of protein solubility from calculation of transfer free energy. *Biophys. J.* **2008**, *95*, 2601–2609.
- (18) Still, W. C.; Tempczyk, A.; Hawley, R. C.; Hendrickson, T. Semianalytical treatment of solvation for molecular mechanics and dynamics. *J. Am. Chem. Soc.* **1990**, *112*, 6127–6129.
- (19) Hawkins, G. D.; Cramer, C. J.; Truhlar, D. G. Parametrized models of aqueous free energies of solvation based on pairwise descreening of solute atomic charges from a dielectric medium. *J. Phys. Chem.* **1996**, *100*, 19824–19839.
- (20) Ghosh, A.; Rapp, C. S.; Friesner, R. A. Generalized Born model based on a surface integral formulation. *J. Phys. Chem. B* **1998**, *102*, 10983–10990.
- (21) Bashford, D.; Case, D. A. Generalized Born models of macromolecular solvation effects. *Annu. Rev. Phys. Chem.* **2000**, *51*, 129–152.
- (22) Lee, M. S.; Feig, M.; Salsbury, F. R., Jr.; Brooks, C. L., III. New analytic approximation to the standard molecular volume definition and its application to generalized Born calculations. *J. Comput. Chem.* **2003**, *24*, 1348–1356.
- (23) Onufriev, A.; Bashford, D.; Case, D. A. Exploring protein native states and large-scale conformational changes with a modified generalized Born model. *Proteins* **2004**, *55*, 383–394.
- (24) Feig, M.; Brooks, C. L. Recent advances in the development and application of implicit solvent models in biomolecule simulations. *Curr. Opin. Struct. Biol.* **2004**, *14*, 217–224.
- (25) Gallicchio, E.; Levy, R. M. AGBNP: an analytic implicit solvent model suitable for molecular dynamics simulations and high-resolution modeling. *J. Comput. Chem.* **2004**, *25*, 479–499.
- (26) Tjong, H.; Zhou, H.-X. GBr⁶: a parameterization-free, accurate, analytical generalized Born method. *J. Phys. Chem. B* **2007**, *111*, 3055–3061.
- (27) Gohlke, H.; Kiel, C.; Case, D. A. Insights into protein-protein binding by binding free energy calculation and free energy decomposition for the Ras-Raf and Ras-RalGDS complexes. *J. Mol. Biol.* **2003**, *330*, 891–913.
- (28) Feig, M.; Onufriev, A.; Lee, M. S.; Im, W.; Case, D. A.; Charles, L.; Brooks, I. Performance comparison of generalized Born and Poisson methods in the calculation of electrostatic solvation energies for protein structures. *J. Comput. Chem.* **2004**, *25*, 265–284.
- (29) Liu, H. Y.; Zou, X. Electrostatics of ligand binding: parameterization of the generalized Born model and comparison with the Poisson-Boltzmann approach. *J. Phys. Chem. B* **2006**, *110*, 9304–9313.
- (30) David, L.; Luo, R.; Gilson, M. K. Comparison of generalized Born and Poisson methods: Energetics and dynamics of HIV protease. *J. Comput. Chem.* **2000**, *21*, 295–309.
- (31) Alsallaq, R.; Zhou, H.-X. Energy landscape and transition state of protein-protein association. *Biophys. J.* **2007**, *92*, 1486–1502.
- (32) Alsallaq, R.; Zhou, H.-X. Prediction of protein-protein association rates from a transition-state theory. *Structure* **2007**, *15*, 215–224.
- (33) Alsallaq, R.; Zhou, H.-X. Electrostatic rate enhancement and transient complex of protein-protein association. *Proteins* **2008**, *71*, 320–335.
- (34) Qin, S.; Zhou, H.-X. Prediction of salt and mutational effects on the association rate of U1A protein and U1 small nuclear RNA stem/loop II. *J. Phys. Chem. B* **2008**, *112*, 5955–5960.

- (35) Zhou, H.-X. A Gaussian-chain model for treating residual charge-charge interactions in the unfolded state of proteins. *Proc. Natl. Acad. Sci. U.S.A.* **2002**, *99*, 3569–3574.
- (36) Hemsath, L.; Dvorsky, R.; Fiegen, D.; Carlier, M. F.; Ahmadian, M. R. An electrostatic steering mechanism of Cdc42 recognition by Wiskott-Aldrich syndrome proteins. *Mol. Cell* **2005**, *20*, 313–324.
- (37) Buckle, A. M.; Schreiber, G.; Fersht, A. R. Protein-protein recognition: crystal structural analysis of a barnase-barstar complex at 2.0-Å resolution. *Biochemistry* **1994**, *33*, 8878–8889.
- (38) Case, D. A.; Darden, T. A.; Cheatham, T. E. I.; Simmerling, C. L.; Wang, J.; Duke, R. E.; Luo, R.; Merz, K. M.; Pearlman, D. A.; Crowley, M.; Walker, R. C.; Zhang, W.; Wang, B.; Hayik, S.; Roitberg, A.; Seabra, G.; Wong, K. F.; Paesani, F.; Wu, X.; Brozell, S.; Tsui, V.; Gohlke, H.; Yang, L.; Tan, C.; Mogan, J.; Hornak, V.; Cui, G.; Beroza, P.; Mathews, D. H.; Schafmeister, J. W.; Ross, W. S.; Kollman, P. A. *AMBER 9*; University of California: San Francisco, 2006.
- (39) Hornak, V.; Abel, R.; Okur, A.; Strockbine, B.; Roitberg, A.; Simmerling, C. Comparison of multiple Amber force fields and development of improved protein backbone parameters. *Proteins* **2006**, *65*, 712–725.
- (40) Ryckaert, J.-P.; Ciccotti, G.; Berendsen, H. J. C. Numerical integration of the Cartesian equations of motion of a system with constraints: molecular dynamics of n-alkanes. *J. Comput. Phys.* **1977**, *23*, 327–341.
- (41) Abdul-Manan, N.; Aghazadeh, B.; Liu, G. A.; Majumdar, A.; Ouerfelli, O.; Siminovitch, K. A.; Rosen, M. K. Structure of Cdc42 in complex with the GTPase-binding domain of the 'Wiskott-Aldrich syndrome' protein. *Nature* **1999**, *399*, 379–383.
- (42) Spencer, D. S.; Xu, K.; Logan, T. M.; Zhou, H.-X. Effects of pH, salt, and macromolecular crowding on the stability of FK506-binding protein: An integrated experimental and theoretical study. *J. Mol. Biol.* **2005**, *351*, 219232.
- (43) Van Duyne, G. D.; Standaert, R. F.; Schreiber, S. L.; Clardy, J. Atomic structure of the rapamycin human immunophilin FKBP-12 complex. *J. Am. Chem. Soc.* **1991**, *113*, 7433–7434.
- (44) Mongan, J.; Case, D. A.; McCammon, J. A. Constant pH molecular dynamics in generalized Born implicit solvent. *J. Comput. Chem.* **2004**, *25*, 2038–2048.
- (45) Cornell, W. D.; Cieplak, P.; Bayly, C. I.; Gould, I. R.; Merz, K. M.; Ferguson, D. M.; Spellmeyer, D. C.; Fox, T.; Caldwell, J. W.; Kollman, P. A. A second generation force field for the simulation of proteins, nucleic acids, and organic molecules. *J. Am. Chem. Soc.* **1995**, *117*, 5179–5197.
- (46) Bondi, A. van der Waals volumes and radii. *J. Phys. Chem.* **1964**, *68*, 441–451.
- (47) Tjong, H.; Zhou, H.-X. GBr⁶NL: a generalized Born method for accurately reproducing solvation energy of the nonlinear Poisson-Boltzmann equation. *J. Chem. Phys.* **2007**, *126*, 195102.
- (48) Schreiber, G.; Fersht, A. R. Interaction of barnase with its polypeptide inhibitor barstar studied by protein engineering. *Biochemistry* **1993**, *32*, 5145–5150.
- (49) Schreiber, G.; Fersht, A. R. Energetics of protein-protein interactions: analysis of the barnase-barstar interface by single mutations and double mutant cycles. *J. Mol. Biol.* **1995**, *248*, 478–486.
- (50) Frisch, C.; Schreiber, G.; Johnson, C. M.; Fersht, A. R. Thermodynamics of the interaction of barnase and barstar: changes in free energy versus changes in enthalpy on mutation. *J. Mol. Biol.* **1997**, *267*, 696–706.

CT8001656